Carbohydrate Research 353 (2012) 79–85

Contents lists available at SciVerse ScienceDirect

Carbohydrate Research

journal homepage: www.elsevier.com/locate/carres

Structural analysis of methyl 6-*O*-benzyl-2-deoxy-2-dimethylmaleimido-α-D-allopyranoside by X-ray crystallography, NMR, and QM calculations: hydrogen bonding and comparison of density functionals

María I. Colombo [a,*], Edmundo A. Rúveda [a], Olga Gorlova [b], Roger Lalancette [b,*], Carlos A. Stortz [c,*]

[a] Instituto de Química Rosario (CONICET-UNR), Facultad de Ciencias Bioquímicas y Farmacéuticas, Suipacha 531, 2000 Rosario, Argentina
[b] Carl A. Olson Memorial Laboratories, Department of Chemistry, Rutgers University, Newark, NJ 07102, USA
[c] Departamento de Química Orgánica-CIHIDECAR, FCEyN-Universidad de Buenos Aires, Ciudad Universitaria, 1428 Buenos Aires, Argentina

ARTICLE INFO

Article history:
Received 31 January 2012
Received in revised form 20 March 2012
Accepted 23 March 2012
Available online 30 March 2012

Keywords:
Allosamine
Conformation
Crystal structure
Density functional theory
N-Dimethylmaleloyl group

ABSTRACT

The crystal structure of methyl 6-*O*-benzyl-2-deoxy-2-dimethylmaleimido-α-D-allopyranoside was solved in order to gain insight into the hydrogen bond features which can be determining features in the glycosylation regioselectivity observed for this compound. An intramolecular hydrogen bond between the hydroxyl H(O)3 and a carbonyl oxygen from the dimethylmaleoyl (DMM) group was observed. This was in agreement with previous NMR temperature shift determinations and molecular modeling. The determination has also found an intermolecular hydrogen bond between the second hydroxyl H(O)4 and the other carbonyl oxygen (generated by symmetry) from DMM. The crystal structure was optimized by five different functionals, namely the hybrid methods B3LYP, M06-2X, B3PW91, and PBE0, and the pure functional PBE, and the optimized geometries were compared with the crystal geometry and with MM3. An excellent coincidence of the geometries was found with the five quantum methods, with minor details deviating from this coincidence. PBE tends to yield larger bond distances, whereas M06-2X fails slightly to match the exocyclic torsion angles for the sugar moiety. In any case, the differences are small, implying that any of these functionals can accurately emulate the geometries of a complex carbohydrate derivative like this one.

1. Introduction

The crucial role of oligosaccharides and derivatives in biological processes has generated a large pressure to synthesize reliably and easily many different carbohydrate oligomers.[1] Thus, glycosylation reactions have drawn much attention from the scientific community, and their stereo- and regio-chemical details, often difficult to predict, were attempted to be rationalized.[2–11] In a previous work,[9] we have shown that *N*-dimethylmaleoyl protected (DMM) D-glucosamine derivatives **1a**, **1b**, **1c** and **2a**, **2b**, **2c**, react with the disarmed glycosyl donors **3** and **4** giving preferential substitution at O3 for the α-glucosides, and mainly O4 substitution for the β-anomers. These results were assessed trying to systematize the influence of the configuration of the anomeric carbons and the effect of the protecting groups on O6 on the relative reactivity. Initially these regioselectivities were rationalized using DFT calculations, which showed that intramolecular H-bonds of H(O)3 with the carbonyl oxygen in DMM for the α-anomer and the H(O)4 with O6 for the β-anomer, could activate their oxygens by increasing their nucleophilicity.[10]

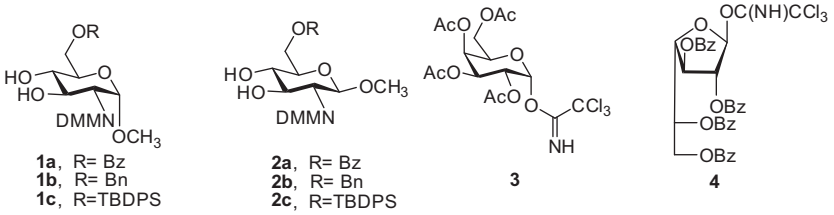

1a, R= Bz
1b, R= Bn
1c, R=TBDPS

2a, R= Bz
2b, R= Bn
2c, R=TBDPS

3

4

* Corresponding authors. Tel./fax: +54 341 43700477 (M.I.C.); tel./fax: +54 11 45763346 (C.A.S.).
E-mail addresses: colombo@iquir-conicet.gov.ar (M.I. Colombo), stortz@qo.fcen. uba.ar (C.A. Stortz).

0008-6215/$ - see front matter © 2012 Elsevier Ltd. All rights reserved.
http://dx.doi.org/10.1016/j.carres.2012.03.025

More recently, however, temperature dependent NMR experiments in DMSO-d_6 solution carried out on the acceptors **1a**, **1b**, **2a,** and **2b** indicated only weak intramolecular hydrogen bonds for their hydroxyl groups.[11] Also, through a series of competition glycosylation experiments of the isomeric acceptors **5**, **6**, **7,** and **8** under standard glycosylation reaction conditions with donor **3**, we established that their reactivities were in the order **7** >> **5** > **8** > **6**, suggesting that a strong intramolecular hydrogen bond is the main requisite to explain the observed trend, and is more important than the axial conformation of the most reactive hydroxyl group.[12]

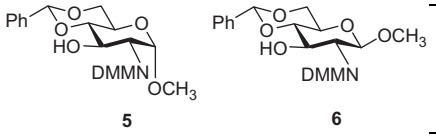

5 **6** **7** **8**

We have established that the hydroxyl proton in the most reactive acceptor **7** participates in a strong H-bond by a study of NMR temperature shifts in DMSO-d_6 solution, and that this bond persists in $CDCl_3$ solution. There are several possible hydrogen acceptors in **7**, such as O1, which would give a classical 1,3-diaxial interaction, or O4, which would lead to an axial/equatorial *cis* 1,2 hydroxy-ether interaction. However, we attributed the H(O)3 bond to the interaction with the CO group of the DMM moiety, on the basis of the lack of hydrogen bonding evidenced for **9 (**missing a DMM group) with an NMR $\Delta\delta/\Delta T$ value of −5.3 ppb/K. Furthermore, quantum mechanical calculations of a simplified analog of **7** confirmed our attribution.[12]

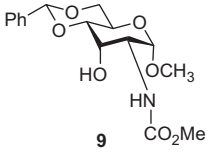

9

To gain further insight into the structure of these and related *N*-dimethylmaleoyl protected hexosamine derivatives, we undertook an X-ray crystal analysis of methyl 6-*O*-benzyl-2-deoxy-2-dimethylmaleimido-α-D-allopyranoside (**10**) recently synthesized in our lab.[11] We selected this compound because it was a key acceptor that allowed us to show that the regioselectivity might be driven by the stabilities of the charged glycosylation reaction intermediates. Furthermore, it carries two OH groups which, on the basis of our observations of the NMR spectra at different temperatures in DMSO-d_6 solution, should show a strong intramolecular H-bond for H(O)3 (−3.5 ppb/K, δ = 5.36 in $CDCl_3$) and a weak one, if at all, for H(O)4 (−7.1 ppb/K, δ = 2.76 in $CDCl_3$).[11] The crystal structure was submitted to DFT optimizations with several different functionals reported to have been used for carbohydrates, and their performances are compared against the crystalline structure.

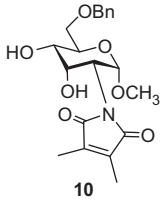

10

2. Methods

2.1. X-ray crystallography

Compound **10** (6-*O*-benzyl-2-deoxy-2-dimethylmaleimido-α-D-allopyranoside) was synthesized as shown elsewhere.[11] A single crystal (colorless plate, 0.49 × 0.44 × 0.21 mm in size) suitable for data collection was mounted on a Cryoloop using Paratone-N, and data were collected on a Bruker SMART ApexII area-detector diffractometer at 100 K.[13,14] The structure was solved using SHELXTL V5.10,[15] SADABS absorption correction was applied,[16] and the determination of the absolute configuration was made as reported by Flack.[17] The radiation source was CuKα, and 16476 reflections were measured. The particulars of the data collection, solution of the structure, and the refinement are given in Table 1, and can be found in the supplemental data (see below).

All H atoms for **10** were found in electron density difference maps. The positions of the two hydroxyl Hs were allowed to vary, but their temperature factors were fixed at U_{iso} (H) = 1.5 U_{eq} (O). The methyl H atoms were put in ideally staggered positions with C–H distances of 0.98 Å and U_{iso} (H) = 1.5 U_{eq} (C). The methylene, methine, and phenyl hydrogens were placed in geometrically idealized positions and constrained to ride on their parent C atoms with C–H distances of 0.99, 1.00, and 0.95 Å, respectively, and U_{iso} (H) = 1.2 U_{eq} (C).

2.2. Calculations

Quantum mechanical (DFT) calculations were carried out using Gaussian 09 W (Rev. B.01)[18] with the basis set 6–31+G(d,p) and standard termination conditions, using the crystal structure as starting point for the first optimization, and the B3LYP optimum geometry for the remaining optimizations. Different functionals were used, namely the hybrid functionals B3LYP,[19,20] B3PW91,[20,21] M06-2X,[22] PBE0[23–25] (also called PBEh, or PBE1PBE), and the pure density functional (generalized gradient approximation) PBE.[23] A small deviation was encountered for the phenyl group with some

Table 1
Crystal data and structure refinement for **10** (6-*O*-benzyl-2-deoxy-2-dimethylmaleimido-α-D-allopyranoside)

Empirical formula	$C_{20}H_{25}NO_7$
Formula weight	391.41
Temperature (K)	100 K
Wavelength (Å)	1.54178 Å
Crystal system, space group	Orthorhombic, $P2_12_12_1$
Unit cell dimensions	a = 10.0296 (4) Å; b = 11.9099 (4) Å; c = 15.9877 (5) Å
Volume (Å^3)	1909.76 (12) Å^3
Z, calculated density	4; 1.361
Absorption coefficient	0.86 mm^{-1}
F (000)	832
Crystal size (mm)	0.49 × 0.44 × 0.21 mm
Θ Range for data collection	4.63; 71.26
Limiting indices	$-12 \le h \le 11$; $-14 \le k \le 13$; $-18 \le l \le 19$
Reflections collected	16,476
Reflections unique	3388
Completeness to θ = 67.7°	97.8%
Maximum and minimum transmission	T_{min} = 0.679, T_{max} = 0.838
Refinement method	Full-matrix least-squares on F^2
Data/restraints/parameters	3388/0/259
Goodness of fit on F^2	1.07
Final R indices	$R[F^2 > 2\sigma(F^2)]$ = 0.028; $wR(F^2)$ = 0.074
Absolute structure parameter	0.02 (13)
Largest difference in peak and hole (e Å^{-3})	$\Delta\rho_{max}$ = 0.20 e Å^{-3}; $\Delta\rho_{min}$ = −0.16 e Å^{-3}

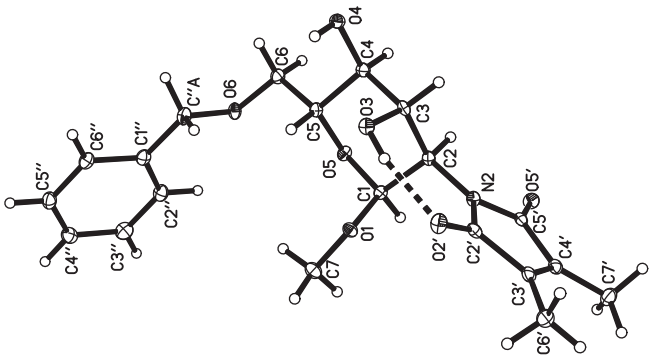

Figure 1. Atom numbering for compound **10** (6-*O*-benzyl-2-deoxy-2-dimethylmaleimido-α-D-allopyranoside). The ellipsoids indicate the regions within which the probability of finding the nuclei is 30%.

of the functionals, thus two different phenyl group conformations were used as starting points for all the quantum mechanical simulations. Molecular mechanics calculations were carried out with MM3(92),[26] modified with sugar parameters as shown elsewhere.[27] The parameters for the dimethylmaleoyl group were adapted from later versions of MM3, from the Tinker parameters,[27] or from extrapolation of parameters for similar atom groups.

2.3. Nomenclature

The numbering scheme of the atoms of **10** is shown in Figure 1. The carbohydrate atoms follow the usual numbering (C1–C6, O1–O6, etc.), with the methyl glycoside carbon as C7. The DMM atoms have primed numbers (C2′–C5′), C2′ being the carbon attached to the oxygen hydrogen-bonded to H(O)3. The DMM methyl groups are numbered as C6′ and C7′. Finally, the benzyl carbon atoms are double-primed numbers (C1″–C6″ and C″A where C2″ is the atom *syn* to O6).

3. Results and discussion

3.1. Crystal and molecular structure details

Details of the structure determination are given in Table 1, whereas the thermal ellipsoid plot with atom numbering is shown in Fig. 1. Final fractional coordinates and U_{eq} values of the atoms are listed in Table 2.

The sugar ring has the usual $^4C_1$ conformation, with puckering parameters[28] *Q*, θ, and ϕ of 0.577 Å, 5.7°, and 261.3°, respectively. As an ideal chair would give $\theta = 0°$, the conformation of this ring is very close to a perfect chair; given the low value of θ, the magnitude of ϕ is not important. As expected, the phenyl and especially the DMM group appear very flat, with puckering amplitudes of 0.0155 and 0.0017 Å. The conformation of the exocyclic methoxyl group on C1 conforms to the expectations of the exoanomeric effect, with a torsion angle ($\chi_{C2-C1-O1-C7}$) of −168.92(11)°.

A strong intramolecular hydrogen bond between H(O)3 and O2′ (carbonyl oxygen of DMM) is observed. The H–O distance is 1.84(2) Å, whereas the distance between both oxygen atoms is 2.6797(15) Å, and the H···O···H angle is 164.9(19)°. All these magnitudes are characteristic of a strong hydrogen bond. A second hydrogen bond, in this case intermolecular, was also found: it occurs between H(O)4 and O5′ (the other carbonyl oxygen of DMM) in a neighboring molecule. This bond is still strong, but weaker than the previous one: the O···O distance is 2.8396(14) Å. In order for the intramolecular hydrogen bond to occur, the DMM group has to tilt with respect to the C2–H2 bond: this has already been previously shown to occur for α-anomers of derivatives with the *gluco* configuration.[10] The degree of tilting

Table 2
Fractional atomic coordinates and isotropic or equivalent isotropic displacement parameters (Å^2)

	x	*y*	*z*	U_{iso}^*/U_{eq}
O1	0.57911 (10)	0.59104 (8)	0.04968 (5)	0.0174 (2)
O3	0.56029 (10)	0.79001 (9)	−0.06066 (6)	0.0181 (2)
H(O)3	0.5867 (19)	0.7341 (17)	−0.0906 (12)	0.027*
O4	0.42996 (11)	0.96080 (8)	0.01424 (6)	0.0198 (2)
H(O)4	0.513 (2)	0.9609 (16)	0.0062 (12)	0.030*
O5	0.41786 (10)	0.69035 (8)	0.12684 (6)	0.0171 (2)
O6	0.50907 (11)	0.83289 (9)	0.25841 (6)	0.0194 (2)
C1	0.44365 (14)	0.61193 (12)	0.06253 (8)	0.0160 (3)
H1	0.3998	0.5394	0.0780	0.019*
C2	0.38168 (13)	0.65327 (11)	−0.01959 (8)	0.0154 (3)
H2	0.2839	0.6581	−0.0080	0.019*
C3	0.42314 (14)	0.77286 (12)	−0.04304 (8)	0.0160 (3)
H3	0.3690	0.7984	−0.0920	0.019*
C4	0.39286 (14)	0.84847 (12)	0.03202 (8)	0.0170 (3)
H4	0.2947	0.8464	0.0428	0.020*
C5	0.46489 (14)	0.80215 (12)	0.10935 (8)	0.0167 (3)
H5	0.5631	0.8002	0.0986	0.020*
C6	0.43711 (15)	0.87192 (12)	0.18692 (9)	0.0194 (3)
H6a	0.4618	0.9510	0.1757	0.023*
H6b	0.3404	0.8697	0.1992	0.023*
C7	0.63931 (15)	0.53248 (13)	0.11797 (9)	0.0229 (3)
H7a	0.6372	0.5799	0.1680	0.034*
H7b	0.7320	0.5145	0.1040	0.034*
H7c	0.5900	0.4629	0.1287	0.034*
C″A	0.64039 (15)	0.87601 (13)	0.26195 (9)	0.0208 (3)
HA″a	0.6371	0.9585	0.2695	0.025*
HA″b	0.6869	0.8601	0.2086	0.025*
N2	0.39429 (11)	0.56873 (10)	−0.08599 (7)	0.0160 (3)
O2′	0.59673 (10)	0.60469 (9)	−0.15291 (6)	0.0228 (2)
O5′	0.19590 (10)	0.47926 (9)	−0.05569 (6)	0.0211 (2)
C2′	0.49823 (14)	0.54699 (12)	−0.14126 (8)	0.0168 (3)
C3′	0.46491 (15)	0.44076 (12)	−0.18662 (8)	0.0186 (3)
C4′	0.34778 (15)	0.40327 (13)	−0.15926 (8)	0.0187 (3)
C5′	0.29897 (14)	0.48340 (12)	−0.09431 (8)	0.0161 (3)
C6′	0.55691 (16)	0.39520 (14)	−0.25151 (9)	0.0242 (3)
H6′a	0.5243	0.3219	−0.2705	0.036*
H6′b	0.6463	0.3866	−0.2276	0.036*
H6′c	0.5606	0.4471	−0.2990	0.036*
C7′	0.26891 (16)	0.30240 (14)	−0.18345 (10)	0.0259 (3)
H7′a	0.1896	0.3259	−0.2147	0.039*
H7′b	0.2416	0.2617	−0.1330	0.039*
H7′c	0.3237	0.2532	−0.2186	0.039*
C1″	0.71655 (16)	0.82376 (13)	0.33336 (9)	0.0202 (3)
C2″	0.67269 (15)	0.72830 (13)	0.37498 (10)	0.0235 (3)
H2″	0.5886	0.6966	0.3612	0.028*
C3″	0.75084 (17)	0.67871 (14)	0.43657 (10)	0.0278 (4)
H3″	0.7199	0.6135	0.4647	0.033*
C4″	0.87367 (16)	0.72427 (14)	0.45697 (9)	0.0255 (3)
H4″	0.9276	0.6897	0.4985	0.031*
C5″	0.91785 (16)	0.82054 (13)	0.41657 (9)	0.0243 (3)
H5″	1.0018	0.8524	0.4305	0.029*
C6″	0.83866 (16)	0.86995 (13)	0.35574 (9)	0.0219 (3)
H6″	0.8684	0.9365	0.3289	0.026*

* The temperature factors for H(O)3 and H(O)4 were fixed at U_{iso} (H) = 1.5 U_{eq} O3 and O4. The methyl H atoms' temperature factors were calculated: U_{iso} (H) = 1.5 U_{eq} (C). The methylene, methine, and phenyl hydrogens' temperature factors were all determined: U_{iso} (H) = 1.2 U_{eq} (C).

of the current DMM group is essentially the same as that determined by QM calculations on an analog of **10**.[12] The C6–O6 group takes a GT conformation (i.e., *gauche* to O5, *trans* to C4), and the phenyl group adopts a conformation practically *syn* to the O6–C″A bond, with a slight deviation (11.3°).

3.2. Molecular modeling of 10

An isolated molecule with the conformation of the crystal structure was submitted to optimization with the most popular density functional, B3LYP, using the basis set 6–31+G(d,p). This basis set was previously deemed as sufficient for geometry determinations of carbohydrates,[29] though some improvements of the energies

Table 3
Selected geometrical features of **10**, obtained for the crystal, and for DFT and MM3 calculations

	Crystal[a]	B3LYP	M06-2X	B3PW91	PBE0	PBE	MM3
Bond lengths (Å)							
C1–O1	1.3964(17)	1.402	1.394	1.396	1.392	1.410	1.418
C2–N2	1.4686(17)	1.470	1.460	1.462	1.458	1.470	1.468
C3–O3	1.4189(17)	1.417	1.410	1.410	1.406	1.423	1.442
C4–O4	1.4173(17)	1.420	1.408	1.412	1.408	1.425	1.436
C5–O5	1.4400(17)	1.442	1.428	1.434	1.429	1.450	1.440
O5–C1	1.4128(16)	1.411	1.400	1.405	1.400	1.419	1.425
O1–C7	1.4293(17)	1.429	1.420	1.421	1.417	1.435	1.432
C1–C2	1.5337(18)	1.543	1.532	1.537	1.534	1.547	1.527
C5–C6	1.5185(18)	1.525	1.516	1.520	1.517	1.527	1.530
Atomic distances (Å)							
H(O)3–O2′	1.838	1.760	1.787	1.741	1.737	1.723	1.860
O3–O2′	2.6797(15)	2.702	2.719	2.685	2.679	2.686	2.728
Bond angles (°)							
C1–C2–C3	113.48(11)	113.7	113.1	113.6	113.5	113.7	112.0
C5–O5–C1	114.2(1)	115.8	114.1	115.3	114.9	114.5	115.5
C1–O1–C7	112.7(1)	113.8	113.0	113.5	113.3	112.9	112.6
O1–C1–O5	113.76(11)	114.0	113.3	114.1	114.0	114.3	109.2
C2–C3–O3	116.49(12)	116.8	116.7	116.7	116.7	116.7	113.0
C6–O6–C″A	112.58(11)	114.3	113.5	114.0	114.0	113.5	114.4
C2–N2–C2′	130.65(11)	130.6	130.1	130.5	130.4	130.5	127.5
N2–C2′–O′	126.89(13)	127.1	127.2	127.1	127.1	127.0	128.2
Torsion angles (°)							
O5–C1–O1–C7	68.37(14)	65.5	58.2	66.0	64.8	65.2	75.3
C1–C2–N2–C2′	−85.41(17)	−84.8	−77.0	−84.5	−83.4	−83.9	−67.7
C2–C3–O3–H	42.3	41.8	30.1	41.1	40.3	40.7	12.1
C3–C4–O4–H	−62.4	−38.8	−40.0	−38.7	−38.5	−38.5	−38.3
O5–C5–C6–O6	63.10(15)	72.6	69.7	72.3	69.1	70.3	63.0
C5–C6–O6–C″A	84.19(15)	85.7	85.3	85.2	84.8	84.0	75.9
C6–O6–C″A–C1″	−174.39(11)	177.9	−171.3	178.3	−174.0	−175.4	175.9
O6–C″A–C1″–C2″	14.41(19)	−12.1	10.7	−9.0	8.6	10.4	61.1
Puckering parameters							
Sugar Q (Å)	0.577	0.561	0.572	0.562	0.564	0.568	0.575
Sugar θ (°)	5.7	5.1	5.3	5.2	5.2	5.6	2.7
DMM Q (pm)	0.17	0.71	2.02	0.70	0.93	0.81	0.53
Phenyl Q (pm)	1.55	0.29	0.25	0.22	0.23	0.26	0.07

[a] Values in parentheses are the errors in the least significant digits.

are observed with higher-level basis sets. The calculations were also carried out with other hybrid functionals, such as B3PW91 and PBE0 which showed better performances (comparing energies) with carbohydrates.[29,30] Calculations were also carried out with a newer (and purportedly better, at least with regular organic molecules[22,31] or nucleic acids[32]) functional like M06-2X, and with the pure generalized gradient approximation (GGA) PBE, also shown to have good performance with carbohydrates.[29] In order to have a calculation control, the minimization was also carried out using MM3, a force-field with strong background in both carbohydrate and regular organic molecules.[26,27]

Although the main conformational features of the crystal structure of **10** are maintained through the optimization processes (see below), the small tilting of the phenyl group with respect to the O6–C″A bond has some particularities: it has a positive value in the crystal, but reverts to a negative (still small) value when calculating with B3LYP and B3PW91. It keeps the positive value with M06-2X, PBE0, and PBE. However, with the two latter functionals, the structure can also be minimized with a negative tilting, giving almost identical energies (less than 0.05 kcal/mol difference). With M06-2X a single minimum is obtained, very close to that observed in the crystal structure. Some selected geometrical data on the crystal structure and the DFT optimizations can be found in Table 3. Each set of data will be analyzed separately.

3.2.1. Bond lengths

The distances for the bonded atoms are quite similar in the crystal and in the vacuum DFT calculations (Table 3). Notable differences are observed, however, especially for the refined O–H bonds, which are quite shorter in the crystal. Even the shortening in the bond distance for the anomeric atoms (particularly C1–O1 and less C1–O5) is very well emulated by the DFT calculations. It should be stressed that previous calculations on model compounds (2-hydroxy- and 2-methoxytetrahydropyran) gave wrong (too large) C1–O1 distances for the axial anomer, using B3LYP with the 6–31G(d) basis set.[27] Evidently, the larger basis set corrects that problem. On the other hand, the C1–O5 distance is well emulated by either basis set. Some functionals tend to give slightly larger distances than the crystal, whereas others tend to give slightly shorter distances. This can be rationalized in terms of Figure 2, which shows the deviation of the calculated distances of each type, with each functional. The plot shows clearly that the deviation for DFT methods rarely exceeds 1% of the actual value. The MM method tends to give larger dispersions, although results are quite acceptable considering the approximations of the method. It can be appreciated that the single C–C bonds are well emulated by the DFT methods with distance ratios very close to 1, and with small dispersion. For sp^2 carbon atoms, the differences are slightly larger, and the DFT methods always give slightly larger distances. For C–C bonds, all the DFT methods give slightly larger distances than the experimental values (Table 4): M06-2X, B3PW91, and PBE0 tend to give more accurate distances (average deviation and standard deviation lower than 0.4%) than B3LYP and PBE (especially the latter, with an average deviation of almost 1%). On the other hand, for the more polar bonds (C–N and single C–O bonds), all relative distances tend to shorten. Thus, the three more accurate functionals for C–C bonds tend to give too short distances (by about 0.5% in average), whereas B3LYP becomes the more

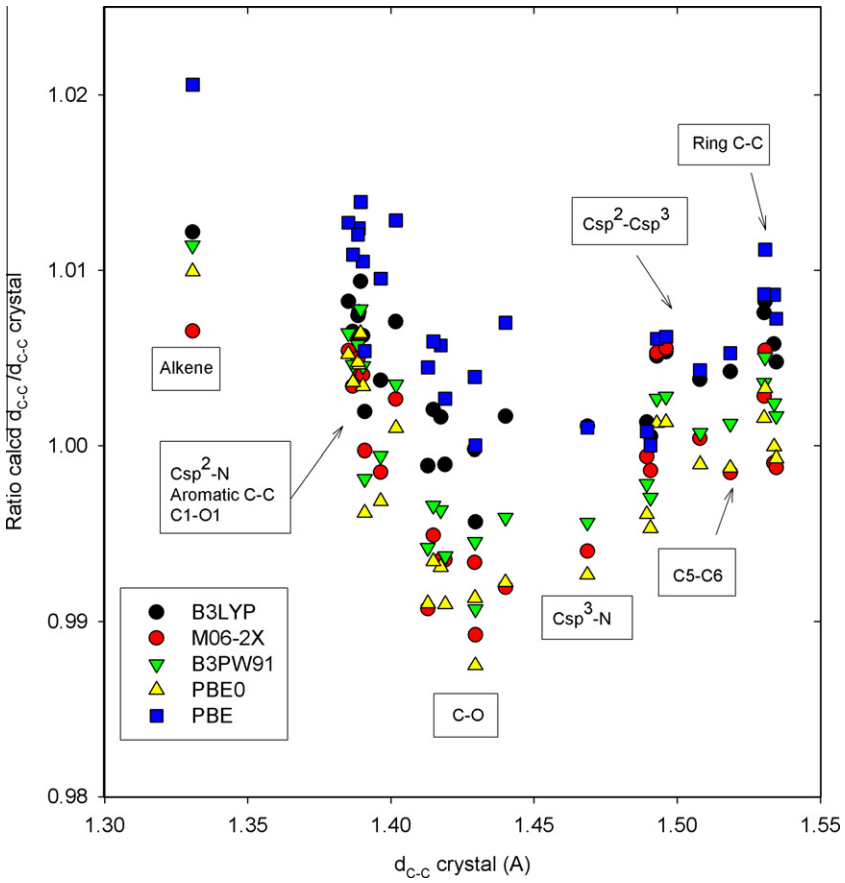

Figure 2. Relationship between the ratio of the DFT, calculated by five different methods, and experimental bond lengths of non-hydrogen atoms against their experimental bond lengths (the region of the C=O is not shown). A value of 1.00 indicates a perfect match between calculated and experimental values.

Table 4
Average ratios and differences between calculated and experimental values

Crystal	B3LYP	M06-2X	B3PW91	PBE0	PBE	MM3
Bond lengths: absolute differences (Å)	0.0068 ± 0.0043	0.0061 ± 0.0045	0.0061 ± 0.0029	0.0065 ± 0.0050	0.0113 ± 0.0068	0.0194 ± 0.0108
C–C Bond lengths ratios	1.0061 ± 0.0028	1.0029 ± 0.0030	1.0036 ± 0.0035	1.0020 ± 0.0038	1.0089 ± 0.0050	0.9939 ± 0.0321
C–X Bond lengths ratios	1.0020 ± 0.0035	0.9954 ± 0.0042	0.9976 ± 0.0045	0.9948 ± 0.0049	1.0070 ± 0.0054	1.0025 ± 0.0121
Bond angles: absolute differences (°)	0.47 ± 0.40	0.48 ± 0.32	0.45 ± 0.34	0.45 ± 0.34	0.42 ± 0.33	1.47 ± 1.19
Bond angles ratios	1.0015 ± 0.0052	0.9996 ± 0.0050	1.0012 ± 0.0048	1.0007 ± 0.0049	1.0007 ± 0.0047	0.9976 ± 0.0160
Torsion angles: absolute differences (°)[a]	2.0 ± 2.3	3.1 ± 3.2	2.0 ± 2.2	1.7 ± 1.5	1.7 ± 1.6	5.5 ± 7.5

[a] Disregarding the torsions around C4–O4 and C1″–C″A.

accurate. PBE still gives large values, indicating that this pure functional tends to overestimate the bond lengths of carbohydrates: this is the only functional giving average absolute differences larger than 0.01 Å (Table 4). As expected, molecular mechanics calculations give larger errors and dispersions. The C5–C6 bond is shorter than the remaining aliphatic C–C bonds, as expected for a GT conformation of the C6 side chain.[33] This shortening is also reproduced by all the DFT methods.

3.2.2. Hydrogen bonds

The intramolecular hydrogen bond between H(O)3 and the carbonyl O2′ is strong according to the experimental X-ray diffraction data (see above). The experimental H···O distance, 1.84(2) Å appears to be shorter by any of the DFT calculation methods (1.723–1.787 Å, Table 3). This can be either due to the observed experimental shortening of the O3–H(O)3 bond (already observed[34,35]), or to a small mitigation of the hydrogen bond strength by the packing forces. When comparing the distance between oxygens O3 and O2′, almost identical calculated (2.679–2.719 Å) and experimental [2.6797(15) Å] values were obtained. The intermolecular hydrogen bond involving H(O)4 was not simulated by the DFT calculations, as they were carried out on single molecules. Thus, no comparison of the data surrounding this atom can be issued.

3.2.3. Bond angles

The regular tetrahedral angle and its expected variations are very well reproduced by the DFT methods (Fig. 3). It is known that the angles around the anomeric region (O1–C1–O5, C5–O5–C1 and C1–O1–C7) are enlarged with respect to the normal tetrahedral angle.[36] This is reproduced by both DFT methods, although B3LYP and B3PW91 tend to overestimate this enlargement, at least for C5–O5–C1 and C1–O1–C7. For axial 2-hydroxytetrahydropyran, the O1–C1–O5 angle is smaller (ca. 111°) either by X-ray diffraction data or by QM calculations..[27,36] The values for the C–O–C angles for that model compound match better with the current ones.

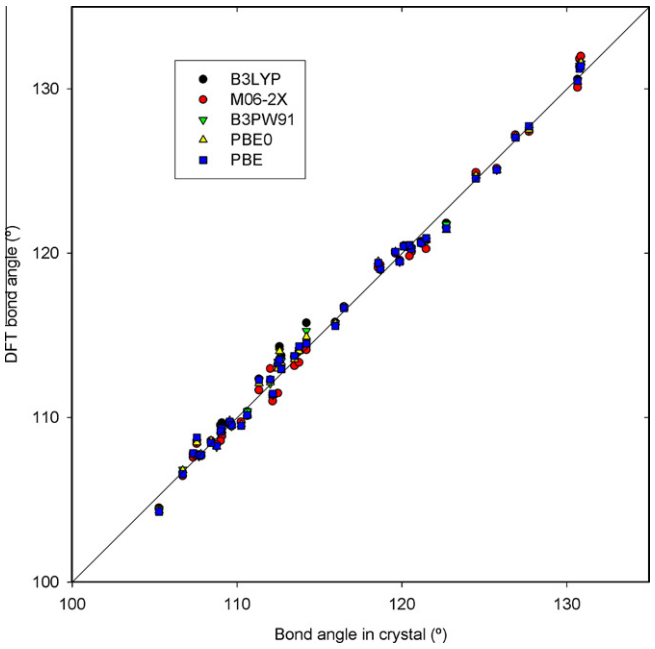

Figure 3. Relationship between the DFT, calculated by five different methods, and experimental bond angles of non-hydrogen atoms. The diagonal line indicates a perfect match between calculated and experimental values.

Other enlargements of the bond angle for the present compound, as occur in C1–C2–C3, C3–C2–N2, C2–C3–O3, and C6–C5–C4 are also very well reproduced by calculations, as does the closure of the angle in C6–C5–O5 and C4–C3–O3. An excellent reproduction is also given by the differential angles of the C2–N2 bond with the two carbonyl carbons, giving rise to a 120° angle with C-5′, and of 130° with C-2′, that with its oxygen engaged in H-bond with H(O)-3. Similar agreements are observed for the DMM and benzyl moieties. Only some discrepancies are found: the C3–O3–H angle fails to reproduce, as occurred with the H-O bond length. Evidently the geometric issues regarding strongly bonded hydrogen atoms are not well reproduced between the crystal diffraction analysis and the calculations. Taking into account just heavy atoms' angles, the one with the largest difference between calculated and crystal corresponds to C6–O6–C″A, especially when using B3LYP (1.7°). However, when the differences are averaged, all the functionals give quite similar values of deviation and dispersion: the average absolute difference of angles is between 0.4 and 0.5° for the five methods. The average ratios are very close to 1, with standard deviations of ca. 0.5%.

3.2.4. Puckering parameters

The assessment of the puckering parameters[28] is a useful quantification of the degree of puckering of the carbohydrate ring. It can also help to determine how planar the other rings (phenyl and DMM) appear. Although these issues can also be tested by comparing the ring torsion angles, puckering parameters provide a simpler comparison. As Table 3 shows, the puckering amplitude (0.561–0.572 Å) and angle θ (5.1–5.6°) calculated by either DFT method match very closely to those determined in the crystal structure (0.577, 5.7°). With these low θ values, there is no point in comparing the phase ϕ angle. On the other hand, the planarity of the DMM and phenyl group is also well reproduced by the DFT calculations, as their *Q* values are very low (Table 3). However, the DFT calculations yield a less flat DMM ring than that determined experimentally, whereas for the phenyl group the reverse behavior is encountered: DFT calculations lead to a flatter ring (Table 3).

3.2.5. Torsion angles

The coincidence of torsion angles between calculated and crystal values is not so straightforward as the previous parameters, depending on each angle and method. This is expected, considering that torsion angles are a softer variable, with less energy compromise than bond lengths or angles. For the dihedrals involving at least two atoms of the carbohydrate ring, the difference in dihedrals between the crystal and the simulated ones are small. This has already been shown previously by way of the puckering parameters. The M06-2X calculation gives the worst results, especially when O5 is involved as the central atom. With the carbohydrate exocyclic dihedrals, less common factors are found: the tilt of the DMM group (necessary for the H-bond to occur) is very well emulated by B3LYP, as shown previously,[10] but also by other functionals like B3PW91, PBE0, and PBE (Table 3). However, M06-2X gives a more pronounced tilt (by about 8°). On the same token, the dihedral around C1–O1, driven by the exoanomeric effect, differs by about 10° with the M06-2X calculation, but only by 3° with the remaining DFT calculations. The same fact occurs with the dihedral around C3–O3, key for the H-bond: M06-2X gives more than 10° difference with the crystal/other DFT determinations (Table 3). These results suggest that M06-2X shows failures to emulate torsion angles around the sugar moiety, as the torsion angles around other organic parts of the molecule are better emulated (Table 3).

The dihedral around C4–O4 is not predicted correctly by any of the calculations, and this makes sense: X-ray diffraction has shown an intermolecular H-bond occurring for H(O)4, which requires a precise conformation of this H atom. As intermolecular interactions are not emulated by the current calculations (which model single molecules in vacuum), the orientation of the H(O)4 is not modeled as expected for a crystal having these interactions. For the ω angle (O5–C5–C6–O6), all DFT calculations overestimate this angle: M06-2X and PBE0 give the lowest overestimation (ca. 6°), whereas B3LYP and B3PW91 give the largest (ca. 9°).

As explained earlier, the phenyl group tilts slightly with respect to the O6–C″A bond (O6–C″A–C1″–C2″ angle, Table 3). This tilt is emulated by M06-2X, PBE0, and PBE, but B3LYP and B3PW91 show a tilt of a similar magnitude but of reverse sign. The presence of this tilt also modifies the torsion angle around the O6–C″A bond (Table 3). MM3 does not emulate properly the position of the phenyl group at all: it takes a transverse position. The average differences in torsion angles (disregarding those around the C1″–C″A and C4–O4 bonds) can be appreciated in Table 4. They show clearly that PBE0 and PBE give the best results, whereas M06-2X gives the worst results in terms of torsion angles.

4. Conclusions

The present study confirms that the strong hydrogen bond between H(O)3 and a carbonyl oxygen from DMM (previously found by NMR temperature shift in DMSO solution and by DFT modeling in vacuum) also exists in the solid state on the α-methylglycoside of a dimethylmaleoylallopyranose protected on C-6 with a benzyl group (**10**). This intramolecular hydrogen bond, crucial to explain the reactivity of this OH in glycosylation reactions, has been detected in acceptors **7** and **10** by NMR temperature shift in DMSO solution and by DFT modeling on a simplified analog of **7**.[11,12] The study also encountered an intermolecular hydrogen bond between H(O)4 and the other carbonyl oxygen from DMM, corresponding to the weak hydrogen bond that had been detected by temperature dependent NMR experiments.[11]

A comparative study of the performance of five different functionals to match the geometry of the crystal structure of **10** showed an excellent coincidence with the five methods, with minor details

favoring one or another in different aspects of the calculation. In any case, the differences are indeed small, and any of these can work nicely to provide information on the geometry of other sugar acceptors that could be potentially useful to rationalize their reactivity, or in any study which requires precise geometry of sugars.

Acknowledgments

This work was supported by Grants from UNR, UBA, ANPCyT, CONICET (M.I.C., E.A.R., and C.A.S.), and NSF-CRIF (0443538) (O.G. and R.L.). M.I.C., E.A.R., and C.A.S. are Research Members of the National Research Council of Argentina (CONICET).

References

1. Zhu, X.; Schmidt, R. R. *Angew. Chem., Int. Ed.* **2009**, *48*, 1900–1934.
2. Whitfield, D. M. *Adv. Carbohydr. Chem. Biochem.* **2009**, *62*, 83–159.
3. Mydock, L. K.; Demchenko, A. V. *Org. Biomol. Chem.* **2010**, *8*, 497–510.
4. Crich, D. *Acc. Chem. Res.* **2010**, *43*, 1144–1153.
5. Bozó, E.; Vasella, A. *Helv. Chim. Acta* **1994**, *77*, 745–753.
6. Muddasani, P. R.; Bernet, B.; Vasella, A. *Helv. Chim. Acta* **1994**, *77*, 334–350.
7. Uriel, C.; Gómez, A. M.; López, C. J.; Fraser-Reid, B. *Eur. J. Org. Chem.* **2009**, 403–411.
8. Cid, M. B.; Alfonso, F.; Alonso, I.; Martín-Lomas, M. *Org. Biomol. Chem.* **2009**, *7*, 1471–1481.
9. Bohn, L. M.; Colombo, M. I.; Pisano, P. L.; Stortz, C. A.; Rúveda, E. A. *Carbohydr. Res.* **2007**, *342*, 2522–2536.
10. Bohn, M. L.; Colombo, M. I.; Rúveda, E. A.; Stortz, C. A. *Org. Biomol. Chem.* **2008**, *6*, 554–561.
11. Colombo, M. I.; Rúveda, E. A.; Stortz, C. A. *Org. Biomol. Chem.* **2011**, *9*, 3020–3025.
12. Colombo, M. I.; Stortz, C. A.; Rúveda, E. A. *Carbohydr. Res.* **2011**, *346*, 569–576.
13. Bruker. *SAINT, Version 7.23a*. Bruker AXS Inc.: Madison, Wisconsin, USA, 2005.
14. Bruker. *APEX 2, Version 2.0-2*. Bruker AXS Inc.: Madison, Wisconsin, USA, 2006.
15. Sheldrick, G. M. *Acta Crystallogr., Sect. A* **2008**, *64*, 112–122.
16. SADABS: *Area-Detector Absorption Correction*; Siemens Industrial Automation, Inc.: Madison, WI, 2008.
17. (a) Flack, H. D. *Acta Crystallogr., Sect. A* **1983**, *39*, 876–881; (b) Flack, H. D.; Bernardinelli, G. *J. Appl. Crystallogr.* **2000**, *33*, 1143–1148.
18. Gaussian 09W, Revision B.01. Frisch, M. J.; Trucks, G. W.; Schlegel, H. B.; Scuseria, G. E.; Robb, M. A.; Cheeseman, J. R.; Scalmani, G.; Barone, V.; Mennucci, B.; Petterson, G. A.; Nakatsuji, H.; Caricato, M.; Li, X.; Hratchian, P.; Izmaylov, A. F.; Bloino, J.; Zheng, G.; Sonnenberg, J. L.; Hada, M.; Ehara, M.; Toyota, K.; Fukuda, R.; Hasegawa, J.; Ishida, M.; Nakajima, T.; Honda, Y.; Kitao, O.; Nakai, H.; Vreven, T.; Montgomery Jr., J. A.; Peralta, J. E.; Ogliaro, F.; Bearpark, M.; Heyd, J. J.; Brothers, E.; Kudin, K. N.; Staroverov, V. N.; Kobayashi, R.; Normand, J.; Raghavachari, K.; Rendell, A.; Burant, J. C.; Iyengar, S. S.; Tomasi, J.; Cossi, M.; Rega, N.; Millam, J. M.; Klene, M.; Knox, J. E.; Cross, J. B.; Bakken, V.; Adamo, C.; Jaramillo, J.; Gomperts, R.; Stratmann, R. E.; Yazyev, O.; Austin, A. J.; Cammi, R.; Pomelli, C.; Ochterski, J.; Martin, R. L.; Morokuma, K.; Zakrzewski, V. G.; Voth, G. A.; Salvador, P.; Dannenberg, J. J.; Dapprich, S.; Daniels, A. D.; Farkas, O.; Foresman, J. B.; Ortiz, J. V.; Cioslowski, J. Gaussian Inc.: Wallington, CT, 2009.
19. Stephens, P. J.; Devlin, F. J.; Chabalowski, C. F.; Frisch, M. J. *J. Phys. Chem.* **1994**, *98*, 11623–11627.
20. Becke, A. D. *J. Phys. Chem.* **1993**, *98*, 5648–5652.
21. Perdew, J. P.; Burke, K.; Wang, Y. *Phys. Rev. B* **1996**, *54*, 16533–16539.
22. Zhao, Y.; Truhlar, D. G. *Theor. Chem. Acc.* **2008**, *120*, 215–241.
23. Perdew, J. P.; Burke, K.; Ernzerhof, M. *Phys. Rev. Lett.* **1996**, *77*, 3865–3868.
24. Adamo, C.; Barone, V. *J. Chem. Phys.* **1999**, *110*, 6158–6170.
25. Ernzerhof, M.; Scuseria, G. E. *J. Chem. Phys.* **1999**, *110*, 5029–5036.
26. (a) Allinger, N. L.; Yuh, Y. H.; Lii, J.-H. *J. Am. Chem. Soc.* **1989**, *111*, 8551–8566; (b) Allinger, N. L.; Rahman, M.; Lii, J.-H. *J. Am. Chem. Soc.* **1990**, *112*, 8293–8307.
27. Stortz, C. A. *J. Comput. Chem.* **2005**, *26*, 471–483.
28. Cremer, D.; Pople, J. A. *J. Am. Chem. Soc.* **1975**, *97*, 1354–1358.
29. Csonka, G. I.; French, A. D.; Johnson, G. P.; Stortz, C. A. *J. Chem. Theor. Comput.* **2009**, *5*, 679–692.
30. Csonka, G. I.; Kaminsky, J. J. *Chem. Theor. Comput.* **2011**, *7*, 988–997.
31. Steinmann, S. N.; Corminboeuf, C. J. *Chem. Theor. Comput.* **2011**, *7*, 3567–3577.
32. Gu, J.; Wang, J.; Leszczinski, J. *Chem. Phys. Lett.* **2011**, *512*, 108–112.
33. Johnson, G. P.; Stevens, E. D.; French, A. D. *Carbohydr. Res.* **2007**, *342*, 1210–1222.
34. Lamba, D.; Segre, A. L.; Fabrizi, G.; Matsuhiro, B. *Carbohydr. Res.* **1993**, *243*, 217–224.
35. Peralta-Inga, Z.; Johnson, G. P.; Dowd, M. K.; Rendleman, J. A.; Stevens, E. D.; French, A. D. *Carbohydr. Res.* **2002**, *337*, 851–861.
36. Rao, V. S. R.; Qasba, P. K.; Balaji, P. V.; Chandrasekaran, R. *Conformation of carbohydrates*; Harwood Academic Publishers: Amsterdam, 1998; pp 91–130.